Published in final edited form as:
J Magn Reson Imaging. 2011 September ; 34(3): 676–684. doi:10.1002/jmri.22647.

Quantitative Contrast-Enhanced First-Pass Cardiac Perfusion MRI at 3T with Accurate Arterial Input Function and Myocardial Wall Enhancement

Elodie Breton, PhD, **Daniel Kim, PhD**, **Sohae Chung, PhD**, and **Leon Axel, PhD, MD**
New York University Langone Medical Center, Center for Biomedical Imaging, 660 First Avenue, New York, NY 10016, USA

Abstract

Purpose—To develop, and validate *in vivo*, a robust quantitative first-pass perfusion cardiovascular MR (CMR) method with accurate arterial input function (AIF) and myocardial wall enhancement.

Materials and Methods—A saturation-recovery (SR) pulse sequence was modified to sequentially acquire multiple slices after a single non-selective saturation pulse at 3T. In each heartbeat, an AIF image is acquired in the aortic root with a short TD (50ms), followed by the acquisition of myocardial images with longer TD values (~150-400ms). Longitudinal relaxation rates ($R_1=1/T_1$) were calculated using an ideal saturation recovery equation based on the Bloch equation, and corresponding gadolinium contrast concentrations were calculated assuming fast water exchange condition. The proposed method was validated against a reference multi-point SR method by comparing their respective R_1 measurements in the blood and left ventricular myocardium, prior to and at multiple time-points following contrast injections, in 7 volunteers.

Results—R_1 measurements with the proposed method and reference multi-point method were strongly correlated ($r>0.88$, $P<10^{-5}$) and in good agreement (mean difference ±1.96 standard deviation 0.131 ± 0.317 / 0.018 ± 0.140 s^{-1} for blood/myocardium, respectively).

Conclusion—The proposed quantitative first-pass perfusion CMR method measured accurate R_1 values for quantification of AIF and myocardial wall contrast agent concentrations in 3 cardiac short-axis slices, in a total acquisition time of 523ms per heartbeat.

Keywords

Magnetic resonance imaging; quantitative myocardial perfusion; R1 relaxation rate; contrast agent; 3T; first-pass perfusion

INTRODUCTION

Contrast-enhanced first-pass perfusion cardiovascular magnetic resonance (CMR) imaging typically acquires 3-4 short-axis images per cardiac cycle, and repeats the acquisition through 40-50 heartbeats during the first passage of a bolus of contrast agent (1-4). Both high spatial (~ 2 mm) and temporal (~ 150 ms) resolutions are necessary to accurately sample the dynamic signal enhancement with minimal partial volume effects and temporal blurring, respectively. Analysis of the resulting images is typically performed qualitatively

Corresponding author: Leon Axel, Ph.D., M.D., Department of Radiology, Center for Biomedical Imaging, New York University School of Medicine, 660 First Ave., 4th floor, New York, NY 10016, Phone: 212-263-6248 - Fax: 212-263-7541, Leon.axel@nyumc.org.

and, hence, is inherently sensitive to reader variability and prone to underestimation of balanced multivessel or diffuse microvascular disease. Quantitative pharmacokinetic analysis of first-pass perfusion CMR images offers the potential to further increase the accuracy of detection of ischemic heart disease. Carrying out such pharmacokinetic modeling requires having accurate values of the dynamic contrast agent concentrations for both arterial input function (AIF) and myocardial enhancement. However, many technical MRI problems must be addressed to convert the observed signal intensities to the corresponding contrast agent concentrations, such as the nonlinear relationship between the MRI signal and contrast agent concentration, ineffective saturation pulses, low signal-to-noise ratio (SNR), and both transmit (B_1+) and receive (B_1−) radio-frequency field inhomogeneities. In addition, AIF and myocardial wall enhancement have different dynamic ranges of T_1, since the concentration of contrast agent passing through the blood being much higher than the net effective concentration passing through the microcirculation in the myocardium. Recent technical advancements towards more quantitative analysis of perfusion CMR images include: dedicated AIF imaging (5-9), robust saturation pulses (10-13), accurate signal-to-concentration modeling (14,15), and higher SNR at 3T (5,16).

The purposes of this work are to: 1) combine the aforementioned advances to develop a robust quantitative first-pass perfusion CMR method able to accurately measure R_1 values for the quantification of AIF and myocardial wall enhancement, and 2) validate *in vivo* the proposed first-pass perfusion CMR method against a reference multi-point saturation-recovery (SR) measurement method at 3T.

MATERIALS AND METHODS

In this study, measurements were expressed in terms of longitudinal relaxation rate ($R_1 = 1/T_1$) because changes in R_1 are linearly proportional to the contrast agent (gadopentetate dimeglumine (Gd-DTPA)) concentration assuming fast water exchange condition (17). The SR time delay (TD) was defined as the time interval between the center of the saturation pulse and the center of the first excitation pulse.

Pulse Sequence

The proposed first-pass perfusion CMR method was developed to accurately image both AIF and myocardial wall enhancement in multiple slices, with the same spatio-temporal resolution, and in a short total acquisition time suitable for high heart rates encountered during cardiac stress testing. An electrocardiogram (ECG)-triggered SR ultrafast gradient echo (i.e., TurboFLASH) pulse sequence was modified to acquire multiple T_1-weighted (T_1w) images with sequential TDs after a single non-selective saturation pulse (18,19) (Fig. 1a), and was implemented on a 3T whole-body MR scanner (Tim Trio, Siemens Healthcare, Erlangen, Germany). This sequential slice acquisition scheme (Fig. 1a) results in a specific T_1-weighting for each imaged slice, which is determined by its TD = TD_1 + TR × (slice number - 1). The proposed first-pass perfusion pulse sequence design consisted of the acquisition of a dedicated AIF image with a short TD (e.g., TD_1 ~ 50-100 ms), followed by 3 myocardial wall images with longer TD values (e.g., $TD_{2\text{-}4}$ ~ 150-400 ms). While the short initial TD value avoids signal clipping at peak contrast agent concentration in the AIF, and is thus suitable for a wide dynamic range of T_1 expected in the blood (~ 50 to 2000 ms), the subsequently longer TD values provide higher SNR and enhancement of the myocardial wall (expected T_1 range ~ 250 to 1500 ms) (7,8). A hybrid adiabatic-rectangular pulse train (10) was used to achieve uniform saturation of magnetization within the whole heart at 3T. Centric k-space reordering was used to minimize the sensitivity to inflow effects (5,20) and to reduce the sensitivity to B_1+ profile after image normalization (21). In the first heartbeat, a proton density-weighted (PDw) image was acquired without the saturation pulse, in order to correct for the spatially varying B_1− and the unknown equilibrium magnetization (14). In

order to minimize T_1-weighting for the PDw acquisition, the imaging flip angle was reduced to 5° and centric k-space reordering was used.

Phantom Validation

Phantom MRI experiments were performed in a wrist CP coil (Siemens Healthcare, Erlangen, Germany), with a simulated ECG-gating set to 60 beats per minute (bpm), in 10 bottles (6 cm in diameter) filled with water doped with different concentrations of Gd-DTPA (0.5M Berlex Magnevist, Schering AG, Germany): 0, 0.05, 0.09, 0.14, 0.22, 0.38, 0.68, 1.05, 2.16 and 4.38 mM. These concentration values were chosen to represent typical R_1 values encountered during a first-pass perfusion CMR examination at 3T (T_1 ~ 50 to 2000 ms, i.e., R_1 ~ 0.5 to 20 s^{-1}). Imaging parameters for the first-pass perfusion SR TurboFLASH pulse sequence included: field-of-view (FOV) = 130 mm × 90 mm, slice thickness 6 mm, matrix = 64 × 44, TE/TR = 1.26/2.42 ms, flip angle 10°, temporal resolution = 106 ms, 4 axial slices, slice distance factor = 100%, and receiver bandwidth = 1008 Hz/pix. The TD values were 50, 156, 263 and 369 ms for slices 1 to 4, respectively. For validation, reference R_1 measurements were made using the multi-point SR TurboFLASH pulse sequence with identical imaging parameters. For each phantom, 20 TD values were chosen to sample the SR curve from approximately $T_1/3$ to $5T_1$.

In Vivo Validation

MRI—First-pass perfusion CMR was performed in 7 healthy volunteers (3 males and 4 females; mean age = 29 ± 11 years), with no known prior history of cardiac disease. Human imaging was performed in accordance with protocols approved by the Human Investigation Committee at our institution; all subjects provided written informed consent. All acquisitions were performed using a 32-element cardiac coil array (Invivo, Orlando, FL). Two repeated first-pass perfusion CMR acquisitions were performed for each volunteer, with the second examination approximately 21 minutes after the first one. We used a low dose (0.05 $mmol.kg^{-1}$) bolus intravenous injection of Gd-DTPA (0.5M Berlex Magnevist, Schering AG, Germany) at an injection rate of 5 mL/s. Imaging parameters for the first-pass perfusion CMR pulse sequence included: FOV = 350 mm × 315 mm, slice thickness 8 mm, matrix = 160 × 144, in-plane resolution 2.2 mm × 2.2 mm, TE/TR = 1.2/2.4 ms, flip angle 10°, temporal resolution = 114 ms, 4 slices, adaptive sensitivity encoding incorporating temporal filtering (TSENSE) (22) parallel acceleration factor 3, and receiver bandwidth = 1008 Hz/pix. The TD values were 50, 164, 278 and 393 ms for slices 1 to 4, respectively. The total acquisition time per heartbeat, including the saturation pulse and acquisition of 4 slices (aortic root perpendicular to the ascending aorta, cardiac short-axis at the basal, mid-ventricular, and apical levels) was 523 ms. The slice acquisition ordering was aortic root followed by short-axis base, mid, and apex in 5 out of 7 volunteers, and aortic root followed by short-axis apex, mid and base in the other 2 volunteers, due to the scanner's automatic slice ordering. For the multi-point SR TurboFLASH acquisition, imaging parameters were kept identical to the single-point first-pass perfusion SR TurboFLASH acquisition, except: FOV = 350 mm × 272 mm, matrix = 144 × 112, in-plane resolution 2.4 mm × 2.4 mm, generalized autocalibrating partially parallel acquisitions (GRAPPA) (23) with an effective acceleration factor 1.7, temporal resolution = 162 ms, and receiver bandwidth = 990 Hz/pix. For each imaging plane, a series of SR images in mid-diastole was acquired within a single breath-hold on the order of 20 s: 1 PDw image, 6 T_1w images with TD ranging from 100 ms to 600 ms (100 ms steps), and an additional 6 T_1w images with TD ranging from 800 ms to 1800 ms (200 ms steps). We assumed that the contrast agent concentration did not change in tissues during the multi-point acquisition.

Validation—The proposed single-point R_1 measurement method was validated *in vivo* against the reference multi-point SR R_1 measurement method. Blood and myocardial R_1

measurements were made in the aortic root and short-axis images, respectively, prior to contrast arrival (baseline) and at multiple time-points following the contrast agent injections, providing 2 sets of R_1 measurements to be compared over a range of contrast agent concentrations (Fig. 1c). Each R_1 comparison time-point consisted of one single-point first-pass perfusion SR acquisition (all 4 slices) inserted between 2 multi-point SR acquisitions (2 different slices), so that the time delay between multi-point and single-point SR acquisitions was minimized (approximately 1 min). In the example shown in Fig. 1c, the first time point indicated (starting 3 min post injection) consisted of a multi-point SR acquisition of slice 1, followed by a single-point "first-pass perfusion" SR acquisition (all 4 slices), which was then followed by multi-point SR acquisition of slice 2. After the subject was given 30 sec to 1 min to rest, the interleaved acquisition scheme was repeated for the remaining 2 imaging planes. The specific slice ordering was pseudo-randomized over time and subjects, in order to minimize possible bias due to the washout of contrast agent during data acquisition. Baseline R_1s were measured prior to any contrast injection. Then, measurements were performed every 3 min up to 21 min after the first contrast agent injection, so that 3 R_1 comparison time-points were obtained per slice. The process was repeated following the second Gd-DTPA injection. A total of 7 R_1 comparison time-points were obtained per slice, which corresponds to 21 and 28 R_1 measurements for the left ventricular (LV) myocardium (i.e., 3 short-axis planes) and blood (i.e., 3 short-axis planes and aortic root plane), respectively, per volunteer. Only 5 and 6, respectively, R_1 comparison time-points were obtained per slice in 2 non-compliant subjects; one subject had breathing artifacts in one of the 2 first-pass perfusion acquisitions and was consequently excluded from the first-pass perfusion analysis. Contours for the myocardium and LV cavity were drawn manually for each image series.

Image Analysis

Single-Point R_1 Measurement—The proposed first-pass perfusion SR method was developed to quantitatively measure R_1 values in the blood and myocardium, in each heartbeat, for the quantification of AIF and contrast agent concentrations in the myocardium. For that purpose, T_1w images were normalized using an extrapolated PDw intensity surface area calculated from a least-square third-degree fit within the user-defined epicardial contour. For the aortic root T_1w images, the smoothed PDw image was used for normalization. A $\sin(\alpha_{PD})/\sin(\alpha_{T_1})$ scaling factor was included in the normalization to account for the different flip angles used in PDw and T_1w image acquisitions, α_{PD} and α_{T1}, respectively. Using the Bloch equation governing T_1 relaxation and centric k-space reordering, with the assumption of a perfectly effective saturation pulse and signal normalization procedure, a simple relationship is obtained between the normalized signal, S^{norm}, and R_1:

$$S^{norm}(R_1, TD) = \frac{S(R_1, TD)}{S^{PD}(R_1, \infty)} \cdot \frac{\sin(\alpha_{PD})}{\sin(\alpha_{T_1})} = 1 - e^{-TD \cdot R_1} \quad [1]$$

where S and S^{PD} are the signal intensities in T_1w and PDw images, respectively.

Multi-Point R_1 Measurement—Reference R_1 measurements were made with a multi-point SR TurboFLASH pulse sequence (24) (Fig. 1b). A series of T_1w images in mid-diastole was acquired, using varying TD and accordingly varied ECG trigger delay (Ttrig) before playing the non-selective saturation pulse. Total acquisition time per image was one heartbeat if TD + acquisition time ≤ one heart beat (Fig. 1b, line 2), or as many heartbeats as necessary if TD + acquisition time > one heart beat (Fig. 1b, line 3). PDw acquisition (without the saturation pulse) was performed in the first heartbeat, with appropriate trigger delay. The Bloch equation governing T_1 relaxation was used to derive a more general

relationship between the signal, S, and R_1, allowing for possible imperfections of the saturation pulse and normalization procedure:

$$S(TD, R_1, S_0, f) = S_0 \cdot \left(1 - [1 - f]\, e^{-TD \cdot R_1}\right) \quad [2]$$

with S_0 the signal of the equilibrium longitudinal magnetization, and f the fraction of the equilibrium longitudinal magnetization that was not effectively saturated by the saturation pulse. A three-parameter (R_1, S_0 and f) nonlinear Levenberg-Marquardt algorithm was used to fit Eq. 2 from the normalized multi-point SR image series.

Signal-to-Concentration Model—Contrast-enhanced first-pass perfusion signal-time curves measured with the proposed pulse sequence were converted to R_1-time curves using equation [1]. R_1-time curves were then converted to Gd-DTPA concentration (*[Gd-DTPA]*)-time curves, assuming fast water exchange condition (17) and a longitudinal relaxivity r_1 = 3.8 L.mmol^{-1}.s^{-1}, as reported at 3T in plasma at 37°C (25-27):

$$[Gd - DTPA] = \frac{\left(R_1 - R_1^{baseline}\right)}{r_1} \quad [3]$$

Note that $R_1^{baseline}$ was measured using the baseline multi-point SR data acquired prior to contrast agent injection.

Data Analysis—Data analysis was performed using custom software developed in MATLAB® (The Mathworks, Inc., Natick, MA). Pearson's linear correlation and Bland-Altman analyses were performed.

RESULTS

The proposed first-pass perfusion CMR method was first validated in phantoms against reference multi-point SR R_1 values. Single-point R_1 values measured in phantoms with the proposed first-pass perfusion SR pulse sequence are plotted against reference multi-point SR R_1 measurements in Fig. 2a, for each TD. Note that R_1 on the order of 20 s^{-1} can be observed in the blood pool at peak enhancement, and that R_1 on the order of 4 s^{-1} can be observed in the myocardium at peak enhancement. Corresponding axial T_1w images of all 10 phantoms, obtained with the proposed first-pass perfusion CMR pulse sequence, are shown Fig. 2.b, for each acquired slice, i.e. for each TD. Note that the geometric changes observed between the imaging planes reflect actual changes in the shape of the bottles used as phantoms. On one hand, measurements with short TD = 50 ms tend to overestimate small R_1 values, due to a lower SNR (e.g., Rician noise bias (28)), but accurately estimate larger R_1 values found at high contrast agent concentrations (Pearson's correlation coefficient (r) > 0.99, p-value (P) < 10^{-5}; slope = 1.00; intercept = 0.27 s^{-1}). On the other hand, single-point R_1 measurements with TD = 156, 263 and 369 ms offer a good estimate of $R_1 < 4$ s^{-1} (r > 0.99, P < 10^{-5}; slope = 1.01, 0.97, 0.94; intercept = −0.01, 0.01, 0.01 s^{-1}, respectively) and are thus well suited for monitoring the myocardial wall enhancement, but they will suffer from signal intensity nonlinearity for higher R_1 values $\left(> \frac{2}{TD}\right)$.

The proposed first-pass perfusion CMR method was validated *in vivo* against multi-point SR R_1 measurements in the blood and myocardium. First-pass perfusion SR single-point R_1 measurements in the blood (TD = 50 ms) and myocardium (TD = 164, 278, 393 ms) are plotted against multi-point SR R_1 measurements in Fig. 3a. Note the difference in dynamic

range between R_1 measured in the LV myocardium (0.6 to 1.6 s^{-1}) and blood (0.3 to 3 s^{-1}), over 3 to 21 min post contrast agent injections. A strong correlation was observed between multi-point and single-point R_1 measurements ($r > 0.88$, $P < 10^{-5}$; slope = 1.01, 1.01, 0.90, 0.82; intercept = 0.12, 0.04, 0.10, 0.15 s^{-1}, respectively for TD = 50, 164, 278 and 393 ms). Corresponding Bland-Altman plots are displayed in Fig. 3b. Mean difference ± 1.96 standard deviation between single-point and multi-point R_1 measurements were 0.131 ± 0.317, 0.041 ± 0.158, 0.023 ± 0.115, −0.011 ± 0.127 s^{-1} for TD = 50, 164, 278 and 393 ms, respectively. As expected in the range of measured R_1 [0.6 - 3] s^{-1}, Bland-Altman analysis showed a non-negligible bias for TD = 50 ms, due to lower SNR in the images compared to longer TD images. There also appeared to be a trend for decreasing myocardium R_1 measurements with increasing TD in the short-axis images, but the shift in mean difference remained within the 95% limits of agreement.

Representative first-pass perfusion CMR images at the aortic root (TD = 50 ms), short-axis basal (TD = 164 ms), mid (TD = 278 ms) and apical (TD = 393 ms) levels are displayed in Fig. 4a. For all 4 imaging planes, the PDw and peak blood and myocardium enhancement T_1w images are shown. Good myocardial contrast enhancement was exhibited in the longer TD short-axis images, even though the dosage was 0.05 mmol/kg. Normalized signal and corresponding R_1 and Gd-DTPA concentration first-pass perfusion time-curves are plotted in the blood (Fig. 4b) and myocardium (Fig. 4c) after the 1st contrast-agent injection in a representative volunteer. Even at peak blood concentration, the peak blood signal was not clipped in the short TD (50 ms) AIF image (Fig. 4b). Normalized signal in the myocardium increased along with TD in the short-axis images (Fig. 4 c). However, similar R_1 values were measured for all 3 short axis images. The final calculation of Gd-DTPA concentrations was made using separately measured baseline R_1.

Pre-contrast R_1 values measured with the multi-point SR fit were 0.509 ± 0.032 s^{-1} in the blood in the aortic root and 0.660 ± 0.036 s^{-1} in the LV myocardium in the short-axis slices. These values are comparable to previously reported R_1 values at 3T (29-31). Peak R_1 and corresponding Gd-DTPA concentrations measured in the blood (aortic root image) and LV myocardium (short-axis images) during the first and second first-pass perfusion CMR are presented in Table 1. These values are consistent with previously reported Gd-DTPA concentrations obtained for a higher dose of 0.1 mmol.kg^{-1} (5,8,15,32).

DISCUSSION

In this study, a quantitative contrast-enhanced first-pass perfusion CMR method is presented and validated *in vivo* at 3T. For the *in vivo* validation, R_1 measurements obtained from the proposed single-point first-pass perfusion method were compared to R_1 measured using the reference multi-point SR method in the blood and myocardium, over a range of contrast agent concentrations. The two methods were strongly correlated and in excellent agreement (Fig. 3). The proposed contrast-enhanced first-pass perfusion CMR method is a promising method to accurately, and time efficiently, measure R_1 values for quantifications of AIF and contrast agent concentrations in the myocardial wall.

Our proposed contrast-enhanced first-pass perfusion CMR method combines a fast multi-slice imaging pulse sequence (19) with robust saturation pulse (10) and accurate dedicated AIF imaging (8,32), signal-to-concentration modeling (14,15), and higher SNR by imaging at 3T (16). The proposed multi-slice pulse sequence follows a strategy similar to previously proposed “dual imaging” sequences, which separately acquire the AIF and myocardial wall enhancement with different R_1 sensitivities (7,8,33). Myocardial wall image acquisitions were performed at long TDs (~ 150-400 ms) in order to achieve higher SNR and good sensitivity to wall contrast enhancement, while AIF acquisition was performed at short TD

(50 ms) in order to avoid signal clipping with high contrast agent concentration in the blood (Fig. 4). The main advantage of the proposed first-pass perfusion CMR pulse sequence is its time efficiency compared with a conventional dual imaging pulse sequence (7,8), i.e., only one saturation pulse module needed per heart beat. For example, the CMR protocol used in this study acquired one AIF and 3 cardiac short-axis images in a total acquisition time per heartbeat that would be suitable for heart rates up to 110 bpm. Our first-pass perfusion CMR protocol can be adjusted for even higher heart rates that might be encountered during a cardiac stress test. Thus, both rest and stress CMR could be acquired with identical spatio-temporal resolution, allowing a direct comparison between rest and stress acquisitions. The acquisition of multiple slices after only one saturation pulse per heartbeat also results in a lower specific absorption rate (SAR) compared to other multi-slice SR pulse sequences. The acquisition of a dedicated AIF image in the ascending aorta, instead of using the blood in the LV cavity, also minimizes the latency between the measured AIF and the actual AIF delivered to the myocardium.

A disadvantage of the proposed pulse sequence is that it generates myocardial wall images with different signal contrasts. A limitation of the method is its sensitivity to to the Rician noise that results in an overestimation of R_1 in low SNR images, i.e., images acquired early during the first passage. This Rician noise bias is TD dependant and primarily affects the short TD AIF images. Correcting for the Rician noise bias was not performed because of the use of parallel imaging (TSENSE), which generates spatially varying (i.e., g-factor) noise. For that reason, baseline R_1 values used in the signal-to-concentration model were measured with the multi-point method. The assumptions used in the simple signal-to-R_1 model include: negligible susceptibility effects of Gd-DTPA (i.e., $T_2^* > TE$), complete saturation of the longitudinal magnetization within the whole heart, perfect spoiling of the residual transverse magnetization after readout, negligible effects of through-plane flow (with centric k-space reordering), negligible effects of B_1- and B_1+ inhomogeneities (with image normalization) and rectangular slice profile. Additional assumptions used to extend the model to a signal-to-concentration model were fast water exchange condition and identical longitudinal relaxivities in the blood and myocardium.

The main limitation of the validation study was that both single-point and multi-point R_1 measurements were made for each effective “time-point”, assuming constant concentration during the acquisitions. However, particularly at short delays after the injection (e.g., 3-5 min), the contrast agent concentration may change significantly over the time needed to actually acquire both datasets (close to 1 minute). To minimize the bias due to contrast agent washout, the acquisition order between single-point and multi-point acquisitions was pseudo-randomized over time and subjects. Another limitation of this study is that the validation experiment was performed during the washout period, and not during the first passage of the contrast agent. As such, maximum contrast agent concentrations that could be measured were small compared to the (rapidly changing) peak concentrations during the first-passage of the bolus (Table 1). The observed tendency for decreasing myocardium R_1 measurements with increasing TD in the short-axis images (Fig. 3 and 4) could be primarily related to the increasing SNR and varying R_1 sensitivities with TD, but also could be related to the signal decrease due to possible excitation crosstalk and magnetization transfer from previous slice acquisitions, and finally to the remaining spatial variation of the saturation pulse efficacy over imaging planes. While the proposed contrast-enhanced first-pass perfusion CMR method was developed and validated in vivo at 3T, it can also be used at 1.5T, at the expense of decreased SNR. The calculated Gd-DTPA concentrations were not validated against actual Gd-DTPA concentrations, which could potentially be measured in simultaneously drawn blood samples. The current study also did not include any imaging under stress nor any patients with ischemic heart disease. Thus, to fully evaluate the clinical utility of this proposed quantitative first-pass perfusion CMR method, additional patient

studies over the whole spectrum of ischemic heart disease encountered in clinical practice will be required.

In conclusion, a contrast-enhanced first-pass perfusion CMR method was developed to time efficiently obtain accurate R_1 values for quantifications of contrast agent concentrations in the blood and myocardium wall. The proposed quantitative first-pass perfusion CMR method was validated *in vivo* at 3T against a reference multi-point SR R_1 measurement method, and it produced both AIF and myocardial wall concentrations consistent with previously published contrast-enhanced first-pass perfusion results.

Acknowledgments

The authors thank Edgar Suan, R.N., for assistance with subject recruitment.

Grant Support: American Heart Association: 0730143N; National Institutes of Health: R01-HL083309, R01-DK069373, R01-EB000447-07A1

REFERENCES

1. Attili AK, Schuster A, Nagel E, Reiber JHC, van der Geest RJ. Quantification in cardiac MRI: advances in image acquisition and processing. Int J Cardiovasc Imaging. 2010; 26:27–40. [PubMed: 20058082]
2. Gerber BL, Raman SV, Nayak K, et al. Myocardial first-pass perfusion cardiovascular magnetic resonance: history, theory, and current state of the art. J Cardiovasc Magn Reson. 2008; 10
3. Jerosch-Herold M, Muehling O. Stress perfusion magnetic resonance imaging of the heart. Top Magn Reson Imaging. 2008; 19(1):33–42. [PubMed: 18690159]
4. Atkinson DJ, Burstein D, Edelman RR. First-pass cardiac perfusion: evaluation with ultrafast MR imaging. Radiology. 1990; 174(3 Pt 1):757–762. [PubMed: 2305058]
5. Kim D. Influence of the k-space trajectory on the dynamic T1-weighted signal in quantitative first-pass cardiac perfusion MRI at 3T. Magn Reson Med. 2008; 59(1):202–208. [PubMed: 17957778]
6. Christian TF, Rettmann DW, Aletras AH, et al. Absolute myocardial perfusion in canines measured by using dual-bolus first-pass MR imaging. Radiology. 2004; 232(3):677–684. [PubMed: 15284436]
7. Gatehouse PD, Elkington AG, Ablitt NA, Yang GZ, Pennell DJ, Firmin DN. Accurate assessment of the arterial input function during high-dose myocardial perfusion cardiovascular magnetic resonance. J Magn Reson Imaging. 2004; 20(1):39–45. [PubMed: 15221807]
8. Kim D, Axel L. Multislice, dual-imaging sequence for increasing the dynamic range of the contrast-enhanced blood signal and CNR of myocardial enhancement at 3T. J Magn Reson Imaging. 2006; 23(1):81–86. [PubMed: 16331593]
9. Hsu LY, Rhoads KL, Holly JE, Kellman P, Aletras AH, Arai AE. Quantitative myocardial perfusion analysis with a dual-bolus contrast-enhanced first-pass MRI technique in humans. Journal of Magnetic Resonance Imaging. 2006; 23(3):315–322. [PubMed: 16463299]
10. Kim D, Oesingmann N, McGorty K. Hybrid adiabatic-rectangular pulse train for effective saturation of magnetization within the whole heart at 3 T. Magn Reson Med. 2009; 62(6):1368–1378. [PubMed: 19785021]
11. Kim D, Gonen O, Oesingmann N, Axel L. Comparison of the effectiveness of saturation pulses in the heart at 3T. Magn Reson Med. 2008; 59(1):209–215. [PubMed: 18050347]
12. Kim D, Cernicanu A, Axel L. B-0 and B-1-insensitive uniform T-1-weighting for quantitative, first-pass myocardial perfusion magnetic resonance imaging. Magn Reson Med. 2005; 54(6): 1423–1429. [PubMed: 16254944]
13. Sung K, Nayak KS. Design and use of tailored hard-pulse trains for uniformed saturation of myocardium at 3 Tesla. Magn Reson Med. 2008; 60(4):997–1002. [PubMed: 18816833]
14. Cernicanu A, Axel L. Theory-based signal calibration with single-point T1 measurements for first-pass quantitative perfusion MRI studies. Acad Radiol. 2006; 13(6):686–693. [PubMed: 16679270]

15. Hsu LY, Kellman P, Arai AE. Nonlinear myocardial signal intensity correction improves quantification of contrast-enhanced first-pass MR perfusion in humans. J Magn Reson Imaging. 2008; 27(4):793–801. [PubMed: 18302205]
16. Cheng ASH, Pegg TJ, Karamitsos TD, et al. Cardiovascular magnetic resonance perfusion imaging at 3-Tesla for the detection of coronary artery disease - A comparison with 1.5-Tesla. J Am Coll Cardiol. 2007; 49(25):2440–2449. [PubMed: 17599608]
17. Donahue KM, Weisskoff RM, Burstein D. Water diffusion and exchange as they influence contrast enhancement. J Magn Reson Imaging. 1997; 7(1):102–110. [PubMed: 9039599]
18. Haase A. Snapshot FLASH MRI. Applications to T1, T2, and chemical-shift imaging. Magn Reson Med. 1990; 13(1):77–89. [PubMed: 2319937]
19. Nagel E, Klein C, Paetsch I, et al. Magnetic resonance perfusion measurements for the noninvasive detection of coronary artery disease. Circulation. 2003; 108(4):432–437. [PubMed: 12860910]
20. Ivancevic M, Zimine I, Montet X, et al. Inflow effect correction in fast gradient-echo perfusion imaging. Magn Reson Med. 2003; 50(5):885–891. [PubMed: 14586998]
21. Breton, E.; Kim, D.; Chung, S.; Axel, L. Theory-based single-point T_1 mapping for quantitative analysis of first-pass cardiac perfusion MRI: a validation study; Proceedings of the 8th Annual Meeting of ISMRM; Stockholm. 2010;
22. Kellman P, Epstein FH, McVeigh ER. Adaptive sensitivity encoding incorporating temporal filtering (TSENSE). Magn Reson Med. 2001; 45(5):846–852. [PubMed: 11323811]
23. Griswold MA, Jakob PM, Heidemann RM, et al. Generalized Autocalibrating Partially Parallel Acquisitions (GRAPPA). Magn Reson Med. 2002; 47(6):1202–1210. [PubMed: 12111967]
24. Wacker CM, Bock M, Hartlep AW, et al. Changes in myocardial oxygenation and perfusion under pharmacological stress with dipyridamole: assessment using T2* and T1 measurements. Magn Reson Med. 1999; 41(4):686–695. [PubMed: 10332843]
25. Pintaske J, Martirosian P, Graf H, et al. Relaxivity of gadopentetate dimeglumine (Magnevist), gadobutrol (Gadovist), and gadobenate dimeglumine (MultiHance) in human blood plasma at 0.2, 1.5, and 3 Tesla. Invest Radiol. 2006; 41(3):213–221. [PubMed: 16481903]
26. Rohrer M, Bauer H, Mintorovitch J, Requardt M, Weinmann HJ. Comparison of magnetic properties of MRI contrast media solutions at different magnetic field strengths. Invest Radiol. 2005; 40(11):715–724. [PubMed: 16230904]
27. Pintaske J, Martirosian P, Graf H, et al. Invest Radiol. 2006; 41(12):859–859. Erratum (vol 41, pg 213, 2006).
28. Gudbjartsson H, Patz S. The Rician distribution of noisy MRI data. Magn Reson Med. 1995; 34(6): 910–914. [PubMed: 8598820]
29. Noeske R, Seifert F, Rhein KH, Rinneberg H. Human cardiac imaging at 3 T using phased array coils. Magn Reson Med. 2000; 44(6):978–982. [PubMed: 11108638]
30. Stanisz GJ, Odrobina EE, Pun J, et al. T1, T2 relaxation and magnetization transfer in tissue at 3T. Magn Reson Med. 2005; 54(3):507–512. [PubMed: 16086319]
31. Sharma P, Socolow J, Patel S, Pettigrew RI, Oshinski JN. Effect of Gd-DTPA-BMA on blood and myocardial T1 at 1.5T and 3T in humans. J Magn Reson Imaging. 2006; 23(3):323–330. [PubMed: 16456820]
32. Elkington AG, He TG, Gatehouse PD, Prasad SK, Firmin DN, Pennell DJ. Optimization of the arterial input function for myocardial perfusion cardiovascular magnetic resonance. J Magn Reson Imaging. 2005; 21(4):354–359. [PubMed: 15779035]
33. Kellman P, Arai AE. Imaging sequences for first pass perfusion - A review. J Cardiovasc Magn Reson. 2007; 9(3):525–537. [PubMed: 17365232]

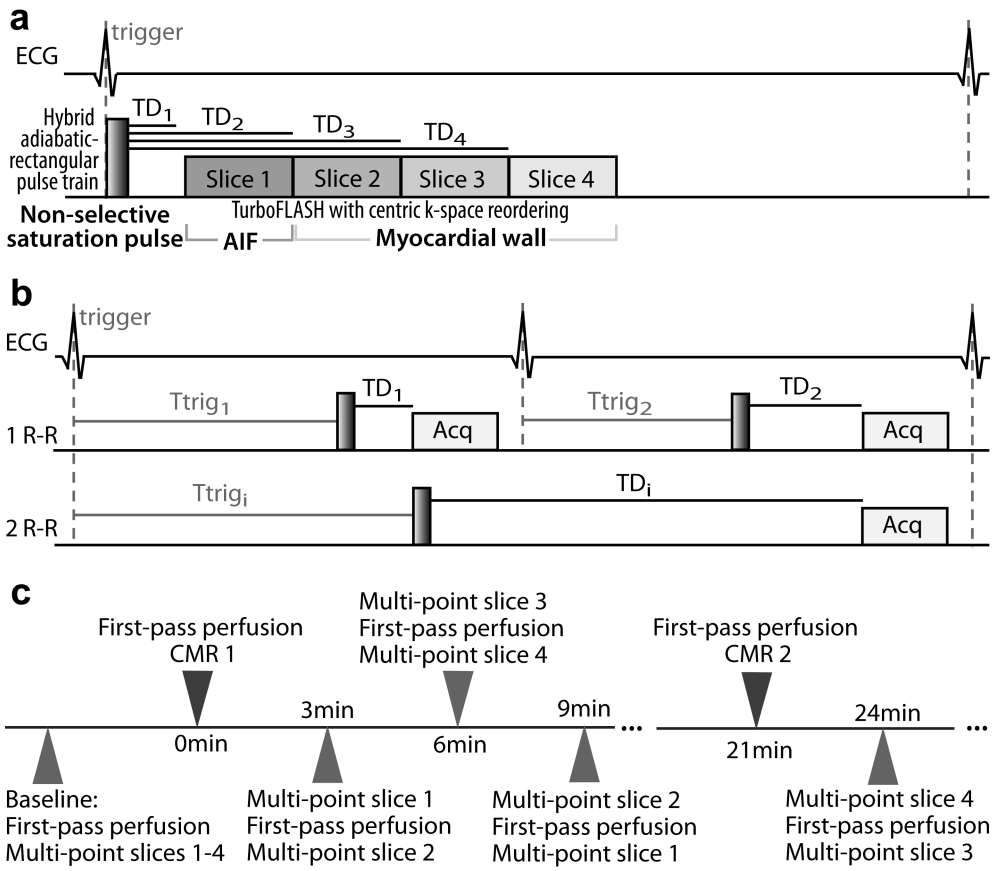

Figure 1.

(a) Schematic pulse sequence diagram of the proposed contrast-enhanced first-pass perfusion CMR acquisition. After a single non-selective saturation pulse (hybrid adiabatic-rectangular pulse train), 4 slices at different locations are sequentially acquired with a TurboFLASH imaging sequence with centric k-space reordering. One AIF image is acquired first with a short TD (e.g., TD_1 ~ 50-100 ms, to avoid signal clipping at peak contrast agent concentrations) followed by 3 myocardial wall image acquisitions with longer TD values (e.g., $TD_{2\text{-}4}$ ~ 150-400 ms, to achieve higher SNR). **(b)** Schematic pulse sequence diagram of the multi-point SR acquisition. A series of T_1w images is acquired in mid-diastole (Acq), using varying TD and ECG trigger delay (Ttrig). Total image acquisition time is one heartbeat if TD + acquisition time ≤ one heart beat (line 2), or as many heartbeats as necessary if TD + acquisition time > one heart beat (line 3). **(c)** Timeline of the *in vivo* validation of the first-pass perfusion CMR method against multi-point SR R_1 measurements. Each comparison "time-point" consisted of one first-pass perfusion CMR acquisition (all 4 slices) inserted between 2 multi-point SR acquisitions (2 different slices). One comparison time-point was acquired every 3 min up to 21 min after each contrast agent injection (6 comparison time-points after each injection, 3 per slice).

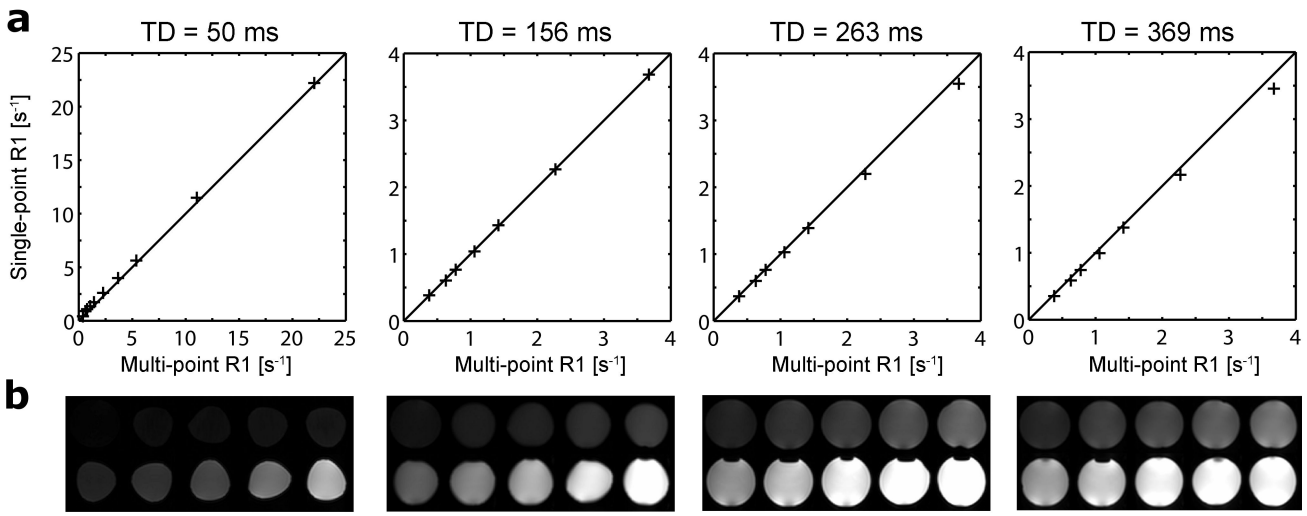

Figure 2.

Phantom validation. **(a)** Single-point R_1 measured using the first-pass perfusion method plotted against reference R_1 from the multi-point SR fit. The black line represents the line of identity. Short TD = 50 ms and longer TD = 156, 263 and 369 ms datasets are presented with different R_1 scale ranges to highlight R_1 sensitivity as a function of TD. **(b)** Corresponding axial T_1w images of all 10 phantoms, obtained with the proposed first-pass perfusion CMR pulse sequence for each TD/slice. Phantoms are shown with R_1 increasing left to right on each row, from top left to bottom right. Note that the geometric changes observed between the imaging planes reflect actual changes in the shape of the bottles used as phantoms.

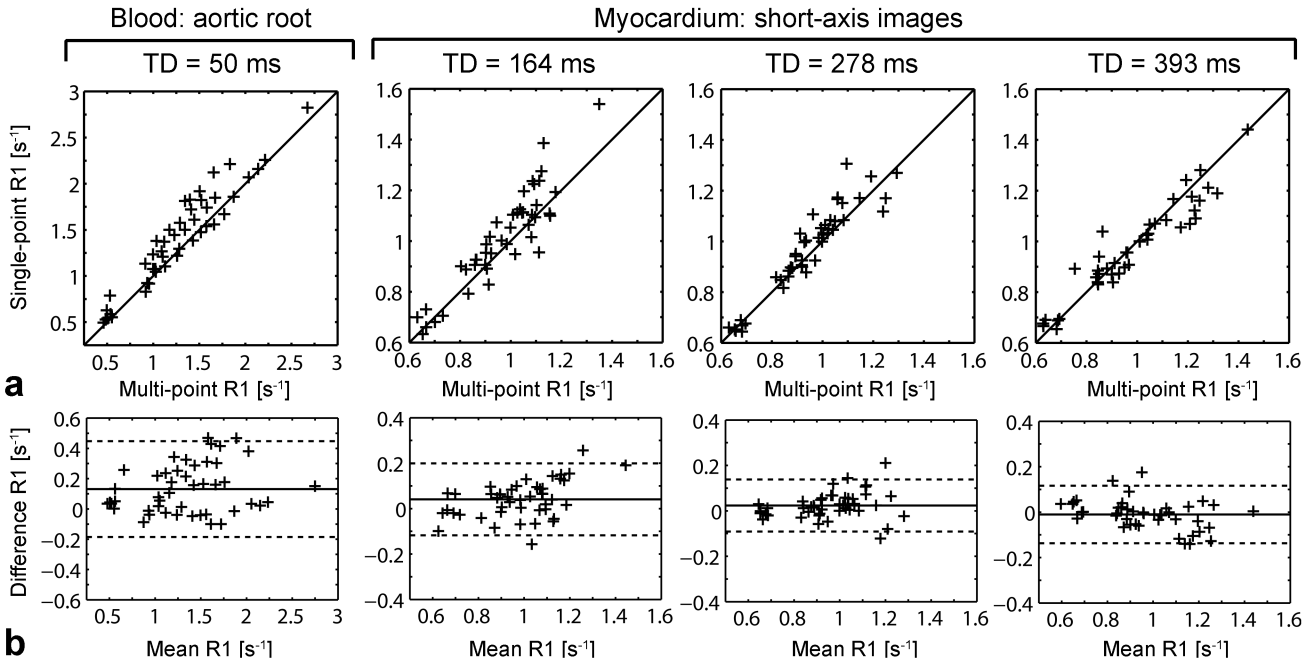

Figure 3.

In vivo validation of the first-pass perfusion CMR method, at baseline and 3 to 21 min after each contrast agent injection. **(a)** Single-point R_1 for each TD/slice plotted against multi-point SR R_1 measured in the blood in aortic root images (TD = 50 ms) and myocardium in short-axis images (TD = 164, 278 and 393 ms). The black line represents the line of identity. **(b)** Corresponding Bland-Altman plots with 95% confidence interval. The mean difference is represented by a plain line, and limits of 95% agreement at mean ± 1.96 standard deviation are plotted as dotted lines.

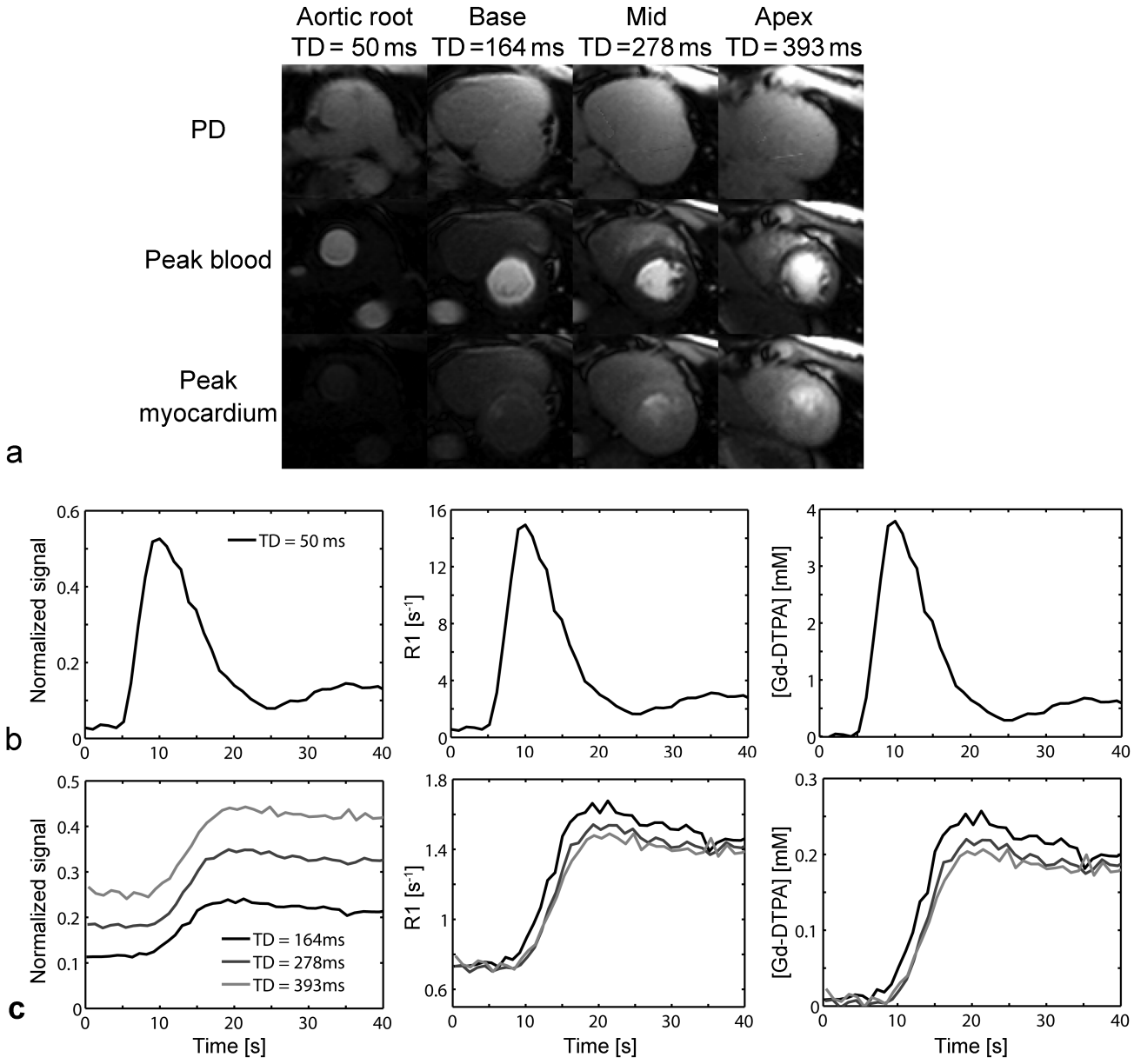

Figure 4.

(a) Representative contrast-enhanced first-pass perfusion SR TurboFLASH single-point images corresponding to PDw, and peak blood and myocardium concentrations, at the aortic root, short-axis base, mid and apex levels. Normalized signal, R_1 and Gd-DTPA concentration ([Gd-DTPA]) first-pass perfusion time-curves in the **(b)** blood (TD = 50 ms) and **(c)** myocardium (TD = 164, 278 and 393 ms) after the 1st injection in a representative volunteer.

Table 1

Peak R_1 and corresponding contrast agent concentration ([Gd-DTPA]) in first-pass perfusion CMR acquisitions

	First-pass perfusion 1		First-pass perfusion 2	
Slice	**R_1 [s^{-1}]**	**[Gd-DTPA] [mM]**	**R_1 [s^{-1}]**	**[Gd-DTPA] [mM]**
Blood: aortic root				
TD = 50 ms	15.494 ± 3.032	3.942 ± 0.803	16.844 ± 3.684	4.298 ± 0.975
Myocardium: short axis				
TD = 164 ms	1.792 ± 0.247	0.294 ± 0.064	2.085 ± 0.267	0.371 ± 0.070
TD = 278 ms	1.680 ± 0.252	0.264 ± 0.067	1.936 ± 0.270	0.332 ± 0.073
TD = 393 ms	1.529 ± 0.164	0.228 ± 0.041	1.956 ± 0.501	0.341 ± 0.128